

PAPER NAME

**Journal\_Amrizal\_ 2013**

AUTHOR

**Amrizal Amrizal**

WORD COUNT

**8264 Words**

CHARACTER COUNT

**41657 Characters**

PAGE COUNT

**11 Pages**

FILE SIZE

**861.7KB**

SUBMISSION DATE

**Dec 3, 2022 4:35 PM GMT+7**

REPORT DATE

**Dec 3, 2022 4:36 PM GMT+7**

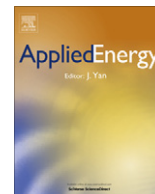
### ● 21% Overall Similarity

The combined total of all matches, including overlapping sources, for each database.

- 20% Internet database
- 9% Publications database
- Crossref database
- Crossref Posted Content database

### ● Excluded from Similarity Report

- Submitted Works database
- Bibliographic material
- Quoted material
- Cited material
- Small Matches (Less than 8 words)
- Manually excluded sources
- Manually excluded text blocks



## Hybrid photovoltaic–thermal solar collectors dynamic modeling

<sup>16</sup> N. Amrizal<sup>a,b</sup>, D. Chemisana<sup>b,\*</sup>, J.I. Rosell<sup>b</sup>

<sup>14</sup> <sup>a</sup>University of Lampung, Bandar Lampung 35145, Indonesia

<sup>14</sup> <sup>b</sup>University of Lleida, c/Pere de Cabrera s/n, 25001 Lleida, Spain

### HIGHLIGHTS

- ▶ A hybrid photovoltaic/thermal dynamic model is presented.
- ▶ The model, once calibrated, can predict the power output for any set of climate data.
- ▶ The physical electrical model includes explicitly thermal and irradiance dependences.
- ▶ The results agree with those obtained through steady-state characterization.
- ▶ The model approaches the junction cell temperature through the system energy balance.

### ARTICLE INFO

#### Article history:

Received 10 April 2012

Received in revised form 27 July 2012

Accepted 14 August 2012

Available online 13 September 2012

#### Keywords:

<sup>3</sup> Hybrid PV/T solar collector  
Thermal characterization  
Electrical characterization  
Dynamical models  
Filtering methods

### ABSTRACT

A hybrid photovoltaic/thermal transient model has been developed and validated experimentally. The methodology extends the quasi-dynamic thermal model stated in the EN 12975 in order to involve the electrical performance and consider the dynamic behavior minimizing constraints when characterizing the collector. A backward moving average filtering procedure has been applied to improve the model response for variable working conditions. Concerning the electrical part, the model includes the thermal and radiation dependences in its variables. The results revealed that the characteristic parameters included in the model agree reasonably well with the experimental values obtained from the standard steady-state and IV characteristic curve measurements. After a calibration process, the model is a suitable tool to predict the thermal and electrical performance of a hybrid solar collector, for a specific weather data set.

© 2012 Elsevier Ltd. All rights reserved.

### 1. Introduction

With <sup>1</sup> solar energy technologies, the hybrid photovoltaic–thermal (PV/T) systems offer an attractive option because the absorbed solar radiation is converted into thermal and electrical energy (the conversion can be done separately or simultaneously). Flat-plate collectors are the most common devices that combine thermal and electrical generation. In order to evaluate these types of collectors, a performance analysis must be undertaken in accordance with the standard test methods available. This can provide objective information, valuable for designers and manufactures in the frame of collector design and system performance optimization for a particular application. Moreover, consumers can also compare the performance and cost-effectiveness ratio of a competing product. Albeit, no dedicated guideline, as a standard test procedure, exists for the performance testing of PV/T flat-plate collectors until now. This field has not been investigated extensively in the litera-

ture. Only a few references refer to PV/T models that can be applied to transient weather conditions.

On the other hand, a wide number of studies associated with the PV/T collectors <sup>1</sup> have been reported in the literature. Most of them are studies about electrical and thermal performances under steady-state conditions [1–3]. Nevertheless, steady-state outdoor testing includes several difficulties associated with the weather conditions. In many places in the world and over many periods throughout the year, the weather conditions do not fulfil the requirements for the steady-state method and long testing periods may be needed to acquire steady-state values. Dynamic or quasi-dynamic characterization methods can offer an effective alternative to overcome these problems. Some representative references regarding quasi-dynamic and dynamic procedures are described below.

Bernardo et al. [4] proposed an empirical model which approaches well the specific thermal power under unstable conditions. However, the specific electrical power predicted by the model showed wider divergences in comparison with the results shown in the thermal part. This system works under concentrated

\* Corresponding author. Tel.: +34 973003711; fax: +34 <sup>18</sup> 3003575.

E-mail address: [daniel.chemisana@macs.udl.cat](mailto:daniel.chemisana@macs.udl.cat) (D. Chemisana).



The theoretical part, Section 2, deals with the model definition and filtering method description. The experimental part includes Sections 3 and 4. The first one concerns the thermal and electrical results and the second one is the discussion of these results. Finally, the main conclusions are stated.

## 2. Theoretical background

### 2.1. The model

The thermal model used in this work is based on the simple dynamical equation presented in the EN 12975 norm (Eq. (H.2)). In order to adapt the model to hybrid PV/T collectors, the solar radiation term has been modified by the useful thermal radiation. The useful thermal radiation,  $G^*$ , is defined as the effective solar radiation which the collector converts into thermal power. Therefore, the radiation fraction transformed into electrical specific power ( $P_{el}$ ) by the PV cells is subtracted to the total solar radiation:  $G^* = G - P_{el}$ . Thus, the useful thermal specific power is expressed as:

$$P_{th} = F'K_0(\theta)(\tau\alpha)_{en}G^* - c_1(T_m - T_a) - c_2(T_m - T_a)^2 - c_5(dT_m/dt) \quad (1)$$

The useful thermal power,  $P_{th}$ , can also be approximated by the following equation:

$$P_{th} = \dot{m}c_p(T_{out} - T_{in})/A_{col} \quad (2)$$

where  $\dot{m}$  is the mass flow rate of fluid,  $c_p$  is the fluid heat capacity,  $(T_{out} - T_{in})$  is temperature difference between fluid outlet and inlet, and  $A_{col}$  is the absorber plate area of the collector.

At this point it should be noted that according to other studies, for example Ref. [1], it is assumed that initially all the solar radiation is converted into thermal energy to obtain the electrical energy fraction. Thus, the useful thermal energy is derived. This treatment does not reflect the physical reality of the system and has a serious drawback: the photovoltaic cell temperature determined is much higher than the real one.

On the other hand, the electrical model employed regards the one stated by Chemisana and Rosell [16]. The useful specific electrical module power is described as:

$$P_{el} = \frac{N_p N_s}{A_{col}} V_c (I_{ph} + I_d + I_{sh}) \quad (3)$$

The model considers recombination losses in the neutral and depletion zones together within the single diode model ( $I_d$ ) and an ideal current source ( $I_{ph}$ ) to implement the photogenerated current and the current losses  $I_{sh}$  complete the model.

The diode current equation is:

$$I_d = I_0 \left[ \exp\left(\frac{V}{nV_T}\right) - 1 \right] \quad (4)$$

The electrical parameterization introduces explicitly the irradiance and temperature dependence of some magnitudes:  $I_{ph}$ ,  $I_0$  and  $nV_T$ . The model assumes that the photocurrent generated  $I_{ph}$  is proportional to the incident irradiance  $G$  and the reverse saturation diode current  $I_0$  has a thermal dependence of  $\varphi(T)$ , where  $\varphi(T) = T_c^3 \exp(-E_g/k_B T_c)$  is the factor depending on the band gap energy  $E_g$  of the cell constituent material, which is considered constant.  $T_c$  is the junction temperature (in K) and  $k_B$  is the Boltzman constant. The temperature dependence of  $E_g$ ,  $I_{ph}$  and  $I_{sh}$  is considered.

The detailed definition of each term used in the model is as follows:

$$I_{ph} = d_1 K_0(\theta)(\tau\alpha)_{en} G \quad (5)$$

$$I_d = d_2 \varphi(T) \left[ \exp\left(\frac{V_c + r_s I_c}{nV_T}\right) - 1 \right] \quad (6)$$

$$I_{sh} = d_3 (V_c + r_s I_c) \quad (7)$$

where  $V_c$  and  $I_c$  are the potential and the current at cell level calculated from the values at the module level in terms of the number of cells connected in series,  $N_s$ , and the number cell lines connected in parallel,  $N_p$  as:

$$V_c = \frac{V}{N_s} \quad (8)$$

$$I_c = \frac{I}{N_p} \quad (9)$$

The specific electrical power stated in Eq. (3), can be approached by:

$$P_{el} = \frac{VI}{A_{col}} \quad (10)$$

In the present research, it is assumed that the cell temperature is the same as the absorber plate temperature. Therefore, it is possible to obtain the cell temperature from the collector parameters as:

$$T_c = T_{in} + \frac{P_{th}}{F'U_L}(1 - F') \quad (11)$$

All these parameters are derived by applying the multiple linear regression process (MLR) on the measured data. This methodology is further described in the next sections.

### 2.2. Data acquisition and filtering methods

In the data acquisition and treatment process act three different time intervals:

- (1) The reading or capturing time interval  $\Delta t_r$ . It is the time when the system collects one data of each measured variable.
- (2) The sampling or measuring interval time  $\Delta t_s$ . It is the interval time when the system saves one averaged value from a certain measured data captured at  $\Delta t_r$ .
- (3) The filtering time interval  $\Delta t_f$ . It is the interval time used to calculate the mean in the moving average technique to reduce high frequency noise. The EN 12975 norm specifies that the reading time interval has to be from 1 to 10 s and the measuring time between 5 and 10 min. There are no other comments in the norm about the filtering interval time and it can be seen that the filtering time is equal to the measuring time.

Regarding the filtering, the Nyquist frequency  $f_N$  is half the sampling frequency (inverse of the sampling time interval) of a discrete signal processing system. The sampling theorem [17] shows that aliasing can be avoided if the Nyquist frequency is greater than the maximum component of the sampling frequency of the signal. In the output temperature of a solar collector the maximum frequency is related with the time constant of the collector  $f_{max} = 1/\tau_c$ , this means that the Nyquist frequency should be at least equal to this value. In consequence, the sampling frequency ( $f_s = 1/\Delta t_s$ ) should be equal or higher than twice this value. The expression in the time domain is:

$$\Delta t_s \leq \frac{\tau_c}{2} \quad (12)$$

And if it is assigned, taking a confidence range  $\Delta t_s = \tau_c/10$  this condition fulfils Eq. (12).

In reference [12] was presented the piston flow model used to simulate the thermal behavior of a collector under dynamical conditions. The results of this research pointed out a linear algebraic expression to calculate the output temperature of the collector as a function of the average value of the radiation and the ambient temperature extended over the response time of the linear model.

The response time of the linear model was defined as:

$$\tau_{lr} = (1 - e^{-1})^{-1} \tau_c \quad (13)$$

where  $\tau_c$  is the collector time constant which is defined as the elapsed time between unshielding the collector to the sun and the point where the collector outlet temperature increases to  $1 - e^{-1}$  (63.2%) from the initial value.

The mean radiation and ambient temperature terms could be understood as the backward moving average for the solar irradiance and the ambient temperature over the response time of the linear model.

In data processing, moving average is a technique used to reduce signal noise. It is used as a low pass filter to eliminate high frequency signal. The cut frequency ( $f_c$ ) is defined as the inverse of the time length used in the average, according to Fourier Analysis. In this case,  $f_c = 1/(\tau_{lr})$ . Hence, signals with frequency higher than the cut frequency are eliminated.

This is the same effect that the collector makes over the meteorological data. If one variable has a change with a frequency higher than the related with the response time of the linear model, in the output the signal is filtered by the dissipative behavior of the thermal effect.

The result of the piston flow model points out that the filtering system based on moving average backwards, extended over a time period equal to the response time of the linear model, is the most appropriated technique that can be used as a filtering process.

### 3. The experimental set-up

The tests were performed in a hybrid PV/T solar collector at the Applied Energy Research Centre (CREA) at the University of Lleida (Spain) which is located in Lleida at latitude 41.36°N and longitude 0.37°E. The data were collected during outdoor tests in November 2011.

The PV/T module consists of 10 lines of 26 series connected crystalline silicon cells optimized for concentrating systems as can be seen in Fig. 1. The cells (NaPFC<sup>®</sup>) are attached to the heat sink, the adhesive used is a material with high heat transfer conductivity that is also resistant to extreme temperatures and is an excellent electrical insulator (Chomerics Thermattach T404). The hybrid absorber is enclosed in an aluminium case with U cross-section; the encapsulation of the collector is finished fixing one top glass cover of 4 mm thickness. The module allows operating under vacuum conditions up to  $10^3$  Pa to improve thermal efficiency. For the present study, the collector was investigated under normal radiation and atmospheric pressure. The main dimensions and characteristics of the collector are summarized in Table 1.

All the instruments and sensors were connected to datalogger CR23X. The inlet and outlet fluid and ambient temperatures, wind speed and solar radiation data were measured using type-K thermocouples, a Vector A-100R cup anemometer and a Kipp & Zonen CMP 11 pyranometer, respectively. The mass flow rate of the working fluid was accurately regulated by using a precision peristaltic pump (Percom N-M) which pumped at a constant known flow rate of 3.17 g/s or 0.022 kg/m<sup>2</sup> s. In order to achieve variations in inlet temperatures during the test, thermostatic immersion circulator (VWR 1122R) capable of water heating with an accuracy of  $\pm 0.1$  °C was used. Measurements were taken for several inlet and outlet fluid temperatures, ambient temperatures, wind speed and solar radiation values. The different input variables were measured every 1 s and their mean values were recorded every 10 s. In parallel and thus, under the same weather conditions, the electrical data were collected employing the IV tracer PVPM 2540C. The system was programmed to collect an IV characteristic curve every 10 min.

In order to have a good comparison with the steady-state results, the dynamic measurements were taken always with the sun perpendicular to the collector. This condition is possible to be reached due to the short measuring time period of time measurements needed as well as the use of a solar tracking system. The data were taken for a fixed low mass flow rate to increase the heat transfer process due to the small surface area of the PV/T collector (Table 1). The same mass flow rate which was applied was kept constant during all the measurement tests.

The thermal experimental procedure conducted, was almost identical to that proposed in the EN. The only difference lies in

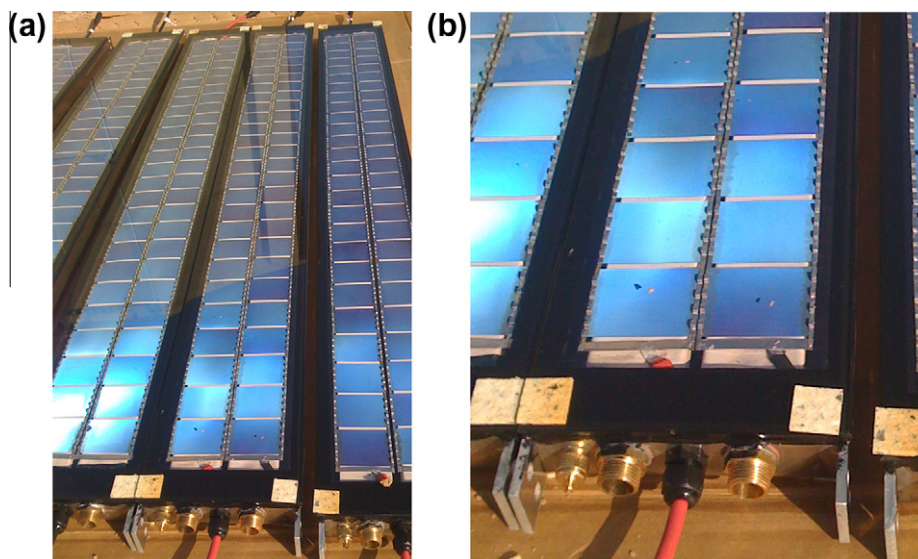


Fig. 1. Picture of the PV/T collectors used in the present work, (b) the connection detail.

**Table 1**  
Data specification of the collectors.

Variable	Value
Mass flow rate (g/s)	3.17
Module area (m <sup>2</sup> )	0.146
Cell area (cm <sup>2</sup> )	16.8
Number of cells connected in series ( $N_s$ )	52
Number of cell lines connected in parallel ( $N_p$ )	1
Volume (l)	0.071
Residence time (s)	22.0
Time constant (s)	87

the fact that the measurements were performed under forced transient conditions. A shading screen was used to fix a constant radiation value in a short time period, instead of measuring during the whole day. In Fig. 2 the collector behavior under these radiation constraints is shown. Two shading Lambertian diffusing screens were used: 1.5 m<sup>2</sup> each; transmittance coefficients: 54.0% and 72.5%, respectively.

### 3.1. Time constant measurement

The measuring of the time constant is needed in the characterization process. As described previously, the time constant determines the time required for the outlet fluid temperature to attain

93.2% of its steady-state value following a step change in the input (Fig. 3). The test method used is in agreement with the procedure described in the EN 12975 standard as presented in Ref. [12]. The final value of the time constant is the average of the values related with four cases with different measurement conditions. These measurements were initially conducted to determine the measured interval time. The measured interval time is defined as the bound period in which the calculations have to be performed. This period reflects the significant duration of the dynamic effect of the collector corresponding to the time derivative of the mean fluid temperature, which was correlated to  $m_e c_e$  term in the quasi-dynamic model as given in Eq. (5).

The effective thermal capacity  $m_e c_e$  and the time constant of the collector are essential parameters in the quasi-dynamic model which characterizes its transient performance. The effective thermal capacity  $m_e c_e$  can be considered as the sum, for each constituent element of the collector (glass, absorber, PV cells, liquid contained, insulation), of the product of its mass, its specific heat and weighting factor. The  $m_e c_e$  can also be calculated from the energy balance of the collector as described in Ref. [13].

### 3.2. Steady-state and dynamical collector characterization

In terms of the dynamic thermal performance characterization, measurements were conducted for collecting data of inlet and out-

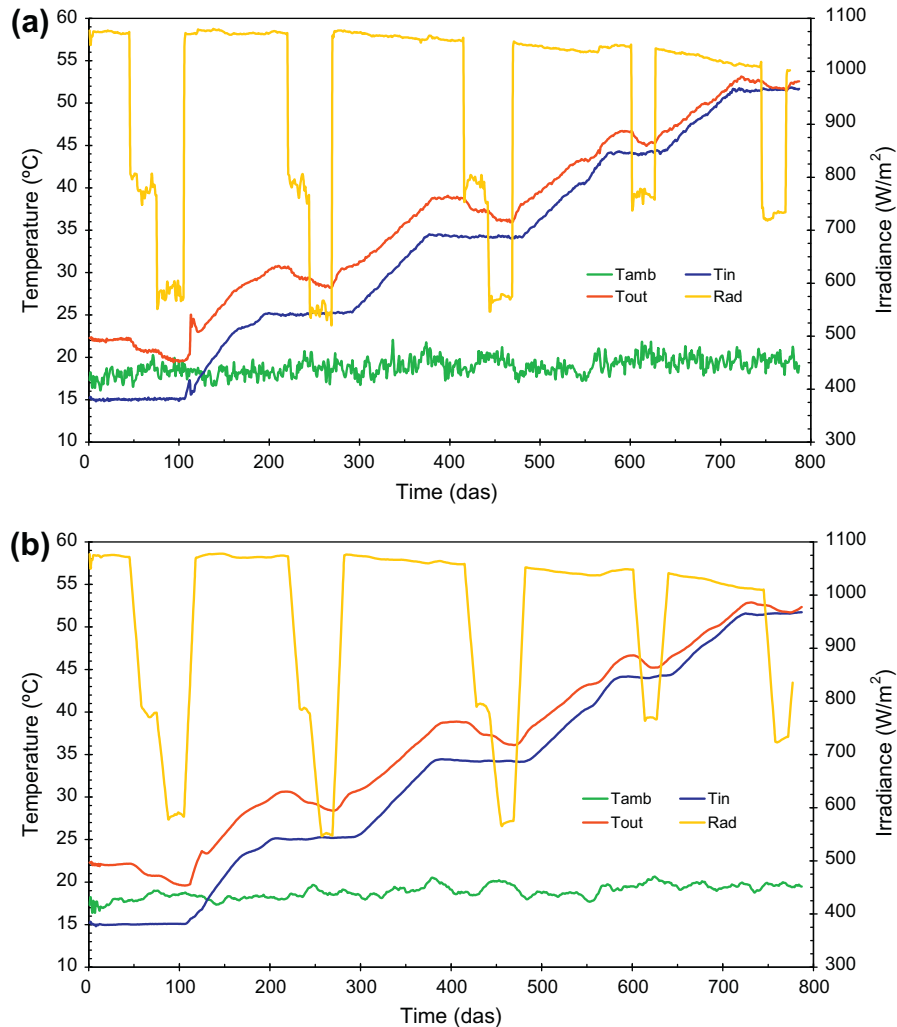


**Fig. 2.** (a) Representation of the experimental data set used to calibrate the model, (b) measured data set with applying moving average techniques. (Time in decaseconds, das)

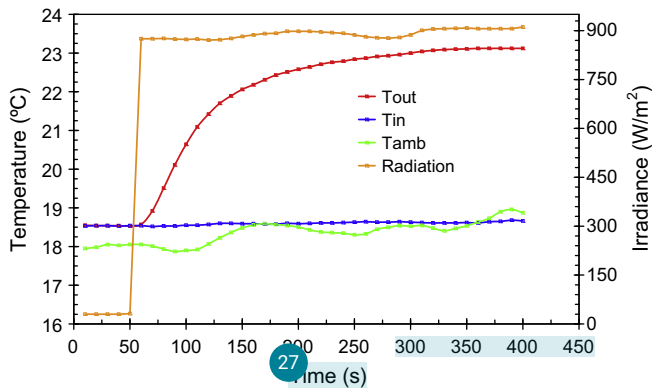


**Fig. 3.** Time evolution of collector outlet fluid temperature  $T_{out}$  during an abrupt radiation change. The shape of the function permits to calculate collector time constant.

let fluid temperatures, ambient temperature, wind speed and solar radiation under forced transient conditions. As mentioned at the beginning of Section 3, in order to perform the measurement process, the collector was faced perpendicular to the sun at around solar noon. The inlet temperature of water was kept constant during five time intervals in the testing, whilst the other values were allowed to vary. Once both inlet and outlet fluid temperatures reached the steady-state conditions, the forced transient condition process was applied by suddenly covering the collector aperture area using the shading Lambertian screen. The collector was shielded for a period equal to four time constants, and then was exposed again to the sun until the next steady-state was achieved. Samples of the measured data are presented in Figs. 2 and 4.

According to the procedure described above, five test sequences were conducted to complete the rating of the collector. Each test corresponded to one over five different inlet fluid temperatures.

One test sequence of measurements has to be conducted with the inlet fluid temperature close to the ambient temperature in order to get the accurate value of zero loss efficiency parameter. The other four measurements have to be performed close to the middle and the highest of the temperature operation respectively. Meanwhile, each of the test sequences was divided into three steps: the *pre-period* to ensure that the steady-state was achieved, the *forced transient period* in which the forced conditions were applied through the shading screen and the *last period* to establish again the steady-state after removing the shading screen (Fig. 2). Each period took 3–4 times the time constant. Therefore, the total time needed for completing test sequence was around 9–12 time constants. Thus, the five tests for the five different inlet temperatures lasted for 27–36 the time constant plus the time required to increase the inlet temperature up to the next level. In this work the total time required was about 130 min.

### 3.3. Electrical measurements – reference characteristic IV curve

The electrical characteristic curve is very sensitive to both the temperature of the photovoltaic cell and the incident solar radiation. The temperature is related to the open-circuit voltage and the irradiance proportional to the short-circuit current (IEC 60904-5, IEC 60891) [18–19]. Accordingly, a reference characteristic IV curve is measured to calibrate the numerical model to refer the  $V_{oc}$  with the corresponding  $T$  and the  $I_{sc}$  with  $G$ .

In the case of the temperature, a problem arises in measuring the  $p-n$  junction temperature and to relate this with the correspondent open-circuit voltage. This is overcome thermalising the PV module at a stable temperature and protecting it from solar radiation. This process can be performed leaving the PV module

in the morning to reach the ambient temperature at around the sunrise, when temperature has variations less than  $\pm 1$  °C/h. For the IV reference curve measurement, once the PV module is connected to the IV tracer, the procedure is as follows: the open-circuit voltage is measured whilst the module is covered, then the module is uncovered and an IV curve is collected, finally the module is covered again to take another  $V_{oc}$  value. These steps must be done as fast as possible to minimize the temperature effect in the measurement. The acquisition of the curve is considered correct if the open-circuit values taken at the beginning and at the end of the test achieve differences less than or equal to 5%.

The determination of the series resistance that appears in Eqs. (6) and (7) is performed according to the methodology presented by De Cueto [20]:

$$\left. \frac{dV}{dI} \right|_{oc} = \frac{n}{V_T} \frac{1}{I_{sc}} + r_s \quad (14)$$

The value of  $r_s$  is obtained by plotting the derivative of the characteristic curve at open circuit conditions in function of the inverse of the short circuit current. The independent term of the linear regression obtained is the  $r_s$  value, as it can be seen in Eq. (14). The rest of electrical parameters are obtained by MLR, as in the thermal characterization.

### 3.4. Parameters identification

In order to facilitate the parameter identification process, the data collection was simplified unplugging the photovoltaic module. Thus, the electrical production was negligible. There was only a small energy extraction when acquiring a characteristic curve about three seconds every 10 min. This simplification allows to firstly identify the thermal parameters. Then, the electrical parameters are determined.

During the experimental test, the data measurement was collected in order to estimate  $P_{th}$  values of the quasi-dynamic model. Multiple linear regression process and moving average (MA) method were applied to the data measurement in order to determine unknown parameters such as  $F(\tau\alpha)_{en}$ ,  $c_1$ ,  $c_2$  and  $c_5$  as given in Eq. (1), where  $F(\tau\alpha)_{en}$  is the zero loss efficiency,  $c_1$  is the heat loss coefficient ( $FU_L$ ),  $c_2$  is the temperature dependence of the heat loss coefficient and  $c_5$  is the effective thermal capacity ( $m_c c_e$ ) respectively.

The MLR method as a mathematical tool which is available in the most standard program with statistical function, was used for the identification of the collector parameters. For an evaluation of the MLR process, all the  $t$ -ratio values of the parameters should be greater than the critical one. If this requirement is not fulfilled, the parameters which indicated with values of less than the critical value should be set to zero and the parameter identification should be repeated with the adjusted collector model. The  $t$ -ratio is calculated as the parameter value divided by the standard error of the same parameter.

As it can be seen in Figs. 2 and 4, the radiation fluctuations in the experimentally measured data obtained in this study were produced by the forced transient conditions. These variations appear jointly with the experimental system noise. The smoothing process is an important tool for reducing the effects of noise in time series. Therefore, the moving average method was applied to the measured data under forced transient conditions [21].

The length of the moving average filter is related with the linear model response time of the collector. As described in Section 2.2, in the present research the linear response time was fixed to be 1.58 collector time constants.

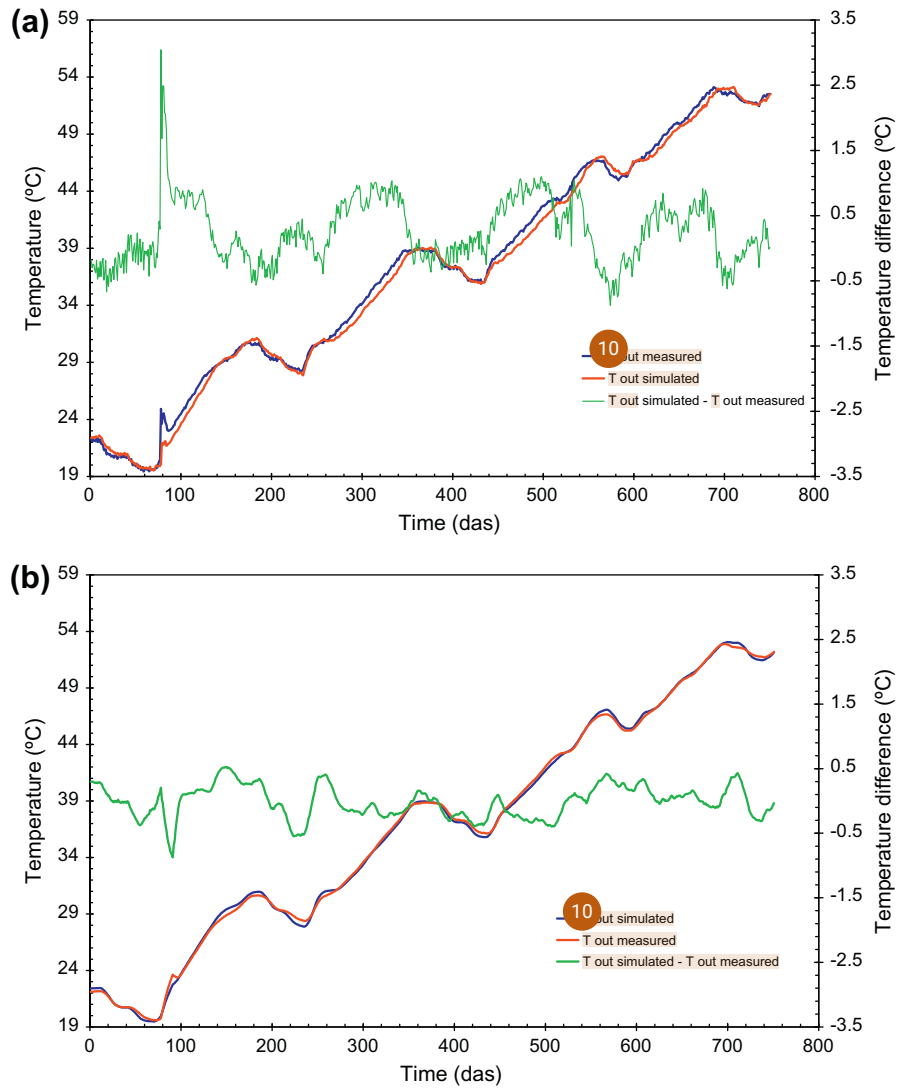


Fig. 4. Time evolution of the measured and simulated output temperatures and the difference between them, (b) time evolution of the measured and simulated output temperatures with the use of moving average and the difference between them.

### 4. Results and discussion

#### 4.1. Time constant and effective heat capacity

Using an initial  $\Delta t_s$  value of 1.0 s, a set of four determinations of the collector time constant corresponding to the four experimental measurements were performed. Fig. 3 shows one of these measurements. It can be observed the exponential behavior of the outlet temperature over time. It is important to notice that in these experiments the water inlet temperature was approximately equal to the ambient temperature while the collector was in thermal equilibrium with both the ambient and the inlet temperatures. The time constant was calculated using the methodology described in Section 3.1. The final value obtained was the mean of the four corresponding determinations,  $\tau_c = 87 \pm 5$  s. This result states that the use of a  $\Delta t_s$  of 10 s is an adequate choice compatible with the specifications mentioned in paragraph 2.2. Consequently,  $\Delta t_r = 1.0$  s was also used. This means that data collection was done capturing data every second and registering the average of the corresponding 10 lectures every 10 s in the datalogger memory.

The time constant also determines the linear model response time by means of Eq. (13) and in the present study takes the value

of 140 s. Therefore, this value has been used as the filtering time interval  $\Delta t_f$  in the backward moving average process.

In agreement with the procedure described in Section 3.1, four effective heat capacity values ( $m_e c_e$ ) were calculated. The average value obtained was found to be  $10.88 \pm 0.19 \text{ kJ m}^{-2} \text{ K}^{-1}$ .

#### 4.2. Model characterization

The data presented in Fig. 3 were used for the collector thermal parameters characterization. These data were collected as described in the methodology discussed in Section 3.2 and by using the time intervals for the data collection obtained in the previous Section 4.1.

Table 2 sums up the steady-state results estimated from the linear regression applied to data obtained only for the intervals during which the inlet temperature remained constant (variation of inlet temperature less than  $\pm 0.5$  °C, as stated in the European Norm; in other words, for the 5 plateau that can be identified in Fig. 2).

An essential validation for the experimental results was the compatibility among steady-state and dynamic. The values obtained by these two tests methods have to be compared within the same parameters. Therefore, the parameters of quasi-dynamic

**Table 2**  
Results from the experimental tests for outdoor steady-state testing.

Parameters	Value $\pm$ SE (95% CI)	t-Ratio value	$r^2$
<i>Steady-state</i>			
$F(\tau\alpha)_{en}$ (-)	$0.635 \pm 0.001$	635	0.9970
$FU_L$ (W/(m <sup>2</sup> K))	$15.2 \pm 1.5$	9.99	
$(m_e c_e)$ (kJ/(m <sup>2</sup> K))	$10.88 \pm 0.19^a$	55.77	

<sup>a</sup> Value calculated from EN 12975 standard (Annex G).

method (Eq. (1)) are used and compared with the parameters of the steady-state model. The results obtained from the steady-state solution are closer to those of the dynamic-state one (Tables 2 and 3). It can also be seen that the coefficient of determination  $r^2$  and the  $t$ -ratio values are quite reasonable for the two test methods. Based on these results, it can be noted that the forced transient conditions could give satisfactory results from three test sequences, which leads to a simple measuring procedure.

On other hand, regarding the forced transient conditions, MLR and MA methods applied in the current work, were acceptable for the dynamic model and for a short time period instead of taking measurements during the whole days. These measurements took much less total time than the measurements during the whole days as performed on the EN 12975 standard.

**Table 3**  
Results from experimental tests for outdoor quasi-dynamic and dynamic testing.

Parameters	Value $\pm$ SE (95% CI)	t-ratio value	$r^2$
<i>Quasi-dynamic</i>			
$F(\tau\alpha)_{en}$ (-)	$0.610 \pm 0.005$	133.31	0.9735
$FU_L$ (W/(m <sup>2</sup> K))	$14.82 \pm 0.21$	72.91	
$(m_e c_e)$ (kJ/(m <sup>2</sup> K))	$6.8 \pm 0.3$	24.07	
<i>Dynamic-state with MA</i>			
$F(\tau\alpha)_{en}$ (-)	$0.641 \pm 0.002$	337.27	0.9959
$FU_L$ (W/(m <sup>2</sup> K))	$15.38 \pm 0.08$	190.12	
$(m_e c_e)$ (kJ/(m <sup>2</sup> K))	$10.62 \pm 0.16$	67.69	

The coefficients for the quasi-dynamic characterization are the same with those for the dynamic one (Table 3), however the dynamic-state coefficients are calculated by using the moving average technique described in Section 2.2 (Eqs. (13) and (14)). The temporal filtering (MA) has been applied not only to the variables  $T_a$  and  $G$ , but it has been extended to the variables  $T_{in}$  and  $T_{out}$  (Fig. 4b). The time interval used in this filter was 140s, which corresponds to  $\tau = (1 - e^{-1})^{-1} \tau_c$ . Another important modification with respect to the EN quasi-dynamic method is the following: for obtaining the above mentioned parameters, all the data recorded including the points with variable  $T_{in}$  were considered. The inclu-

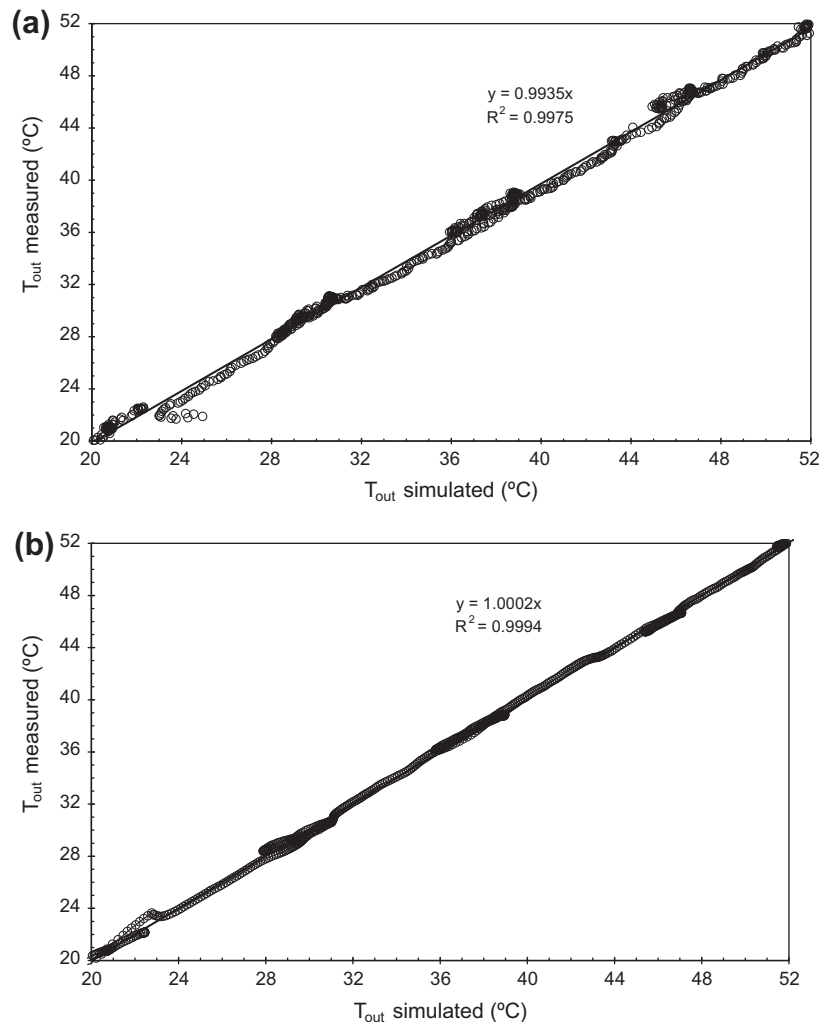


**Fig. 5.** Measured outlet temperatures  $T_{out}$  vs. the modeled ones: (a) without applying the MA technique, (b) with applying the MA technique.

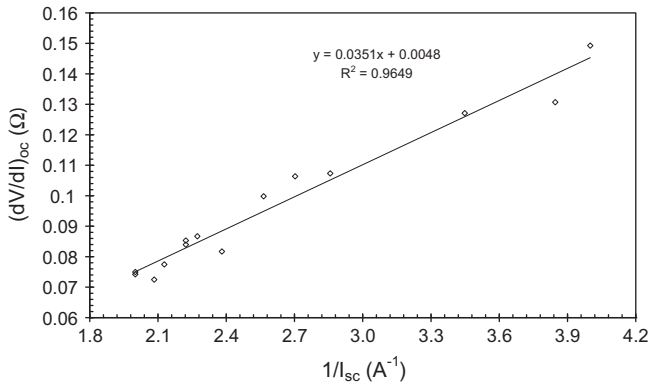


Fig. 6. Cell electrical resistance  $R_{oc}$  ( $dV/dI$ ) $_{oc}$  vs. the inverse of the short circuit cell current ( $1/I_{sc}$ ).

sion of these new items improved in all cases the statistical descriptors used for the evaluation of the methodology.

The most significant difference introduced by using the moving average technique is the stabilization of the obtained effective heat capacity value. As remarked in the introduction and reported in the literature, one of the major drawbacks of using the quasi-dynamic standard method is the variability of the values obtained by the linear regression. From the results presented in Tables 2 and 3, it can be noted that the numbers obtained through the proposed procedure are the closest determinations achieved in reference to the measurements collected. The relative discrepancy of the effective heat capacity with respect to the experimental data was 62.9% for the standard method and 1.5% for the proposed method.

After adjusting the parameter in the identification process, all the  $t$ -ratio have an absolute value greater than the critical one, therefore this means that all the parameters in the regression equation are useful in predicting the assessed value of the quasi-dynamic model.

The results calculated for the outlet temperature are plotted in Fig. 4a for the standard method and in Fig. 4b for the proposed

method using the moving average technique. In both cases the simulated temperature was calculated using an iterative process (Eq. (1)) and setting  $P_{el} = 0$ . In Fig. 5 the comparison between the outlet experimental temperatures and modeled ones obtained from both methods, is depicted. The moving average provides a better estimate than the original values because noise is reduced. The measured data fluctuations were smoothed to expose its features and provide a reasonable starting approach for parametric fitting.

Fig. 7 plots a set of the most representative experimental  $I$ – $V$  curves corresponding to different irradiances and temperatures (circles). Each curve is represented by 100 measured points.

From the experimental  $I$ – $V$  values and following the methodology described in Section 3.4, the resistance under open circuit conditions  $r_{oc}$  was calculated. Fig. 6 shows the correlation between the resistances  $r_{oc}$  and the inverse short circuit currents obtained under the same weather conditions. In Fig. 6, the linear equation which best correlates both variables, is also presented. The y-interception of the equation found, according to Eq. (14), represents the value of the mean series resistance  $r_s$  of an average cell of the module. In this case  $r_s = 0.7 \text{ m}\Omega$ .

The constants  $d_1$ ,  $d_2$  and  $d_3$  were determined by fitting Eq. (2) to the experimental data. The results of the three constants, the series resistance and the ideality factor are given in Table 4. The goodness of the fit can be appreciated graphically in Fig. 7, where a set of measured curves is plotted against the simulated values obtained by substituting the parameters from Table 4 in Eq. (2). Using the same temperature and irradiance values, the slope obtained was almost 1 while the coefficient of determination was 0.999 (Fig. 8). From the  $t$ -Student parameter analysis, all the parameters achieve a  $t$ -value above the critical so they have significance in defining the final value.

Fig. 9 shows the comparison between the average cell temperature determined experimentally and the one calculated by Eq. (10). In Fig. 9, the results from applying the same equation to particular input values, such as the mean fluid, the outlet and the inlet temperatures. This figure demonstrates that the inlet temperature is the one which best adjusts the cell temperature.

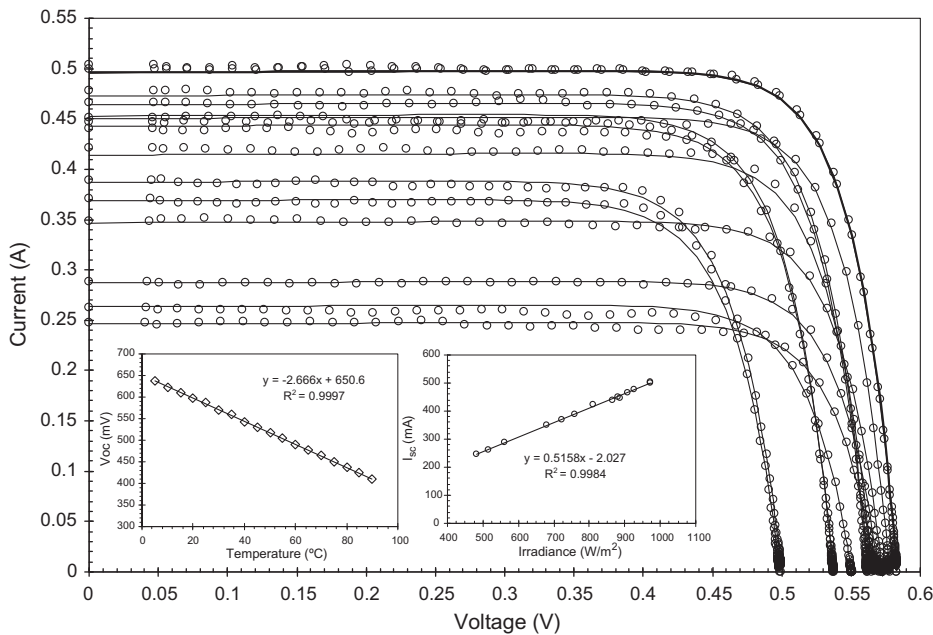
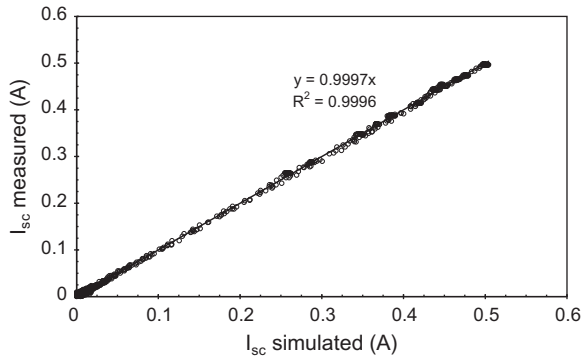


Fig. 7. Set of experimental and simulated representative electrical IV characteristic curves for solar radiation  $G$  ranging from 500 to 1050  $\text{W m}^{-2}$  and cell temperature  $T_c$  ranging from 17 to 45 °C. This set of data was used to derive the electrical parameters from the model.

**Table 4**  
Cell electrical coefficients.

	$d_1$ ( $\text{Am}^2 \text{W}^{-1}$ )	$d_2$ ( $\text{AK}^{-3}$ )	$d_3$ ( $\Omega^{-1}$ )	$n$ (-)	$r_s$ ( $\Omega$ )
Value	$5.14 \times 10^{-4}$	-731.02	$-9.75 \times 10^{-3}$	1.19	$7.45 \times 10^{-4}$
Standard error	$1.41 \times 10^{-6}$	2.41	$3.24 \times 10^{-3}$		



**Fig. 8.** Correlation between the simulated and experimental currents. The simulated values were obtained from Eqs. (2)–(8) and by using the coefficients given in Table 4.

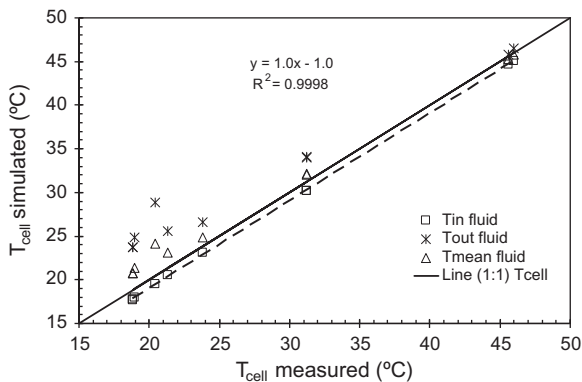


**Fig. 9.** Results for the cell temperature obtained by Eq. (1) using different values of input temperature compared with the experimental values.

**Table 5**  
Electrical characteristics at standard conditions (25 °C and 1.0  $\text{kWm}^{-2}$ ).

	Average cell	Module
$V_{oc}$ (V)	0.586	30.51
$I_{sc}$ (A)	0.510	0.510
$P_{mp}$ (W)	0.241	12.53
$V_{mp}$ (V)	0.500	26.00
$I_{mp}$ (A)	0.483	0.483
$\eta$ (%)	14.3	8.55
FF (-)	0.802	0.802

It is noteworthy that the electrical characterization performed provides a good description of the collector behavior as photovoltaic module for any working condition. This amplifies significantly the photovoltaic characterization methodology defined under the standard IEC 60904 [18]. As described in the standard, the characterization is carried out only under determined environmental conditions (standard conditions STC). These conditions are extended approximately to other conditions by using the  $T_{NOC}$  equation and by introducing other thermal parameters such as alpha and beta [22], sometimes not measured directly on the module,

depending on its manufacturing technology. Finally, the main electrical characteristics for the cell and for the module are given in Table 5. In the efficiency calculation, the PV cell coverage ratio obtained by dividing the cell area by the module area (0.598), is used to relate both the cell and the module values [23].

## 5. Conclusions

In this paper, a modified test to characterize the behavior of a PVT solar collector was developed and carried out. The model presented an extension and coupling of the quasi-dynamic thermal test with the single-diode photovoltaic model. The joining term is the effective solar radiation delivered on the thermal absorber.

The forced transient conditions were applied to the incoming solar radiation in order to increase the thermal capacitance effect and the thermal variability. This led to a simpler process and a shorter test period for quasi-dynamic performance tests. The forced conditions were achieved through the use of a Lambertian screen.

An adequate sampling interval time and the backward moving average technique used allow reduction of the heat capacity fluctuations, and thus the linear regression results are improved considerably. Besides, this permits to model the system with no constant inlet temperature requirements. The sampling interval time was set to be approximately 1/10 the time constant. The filter length used in the moving average was fixed to 1.58 times the collector time constant.

The electrical parameterization introduced explicitly the irradiance dependence of the photogenerated current and the thermal dependence of the reverse saturation diode current. Contrarily, no temperature dependence in the gap energy and photogenerated current was considered.

The electrical performance had been analyzed through the  $I$ - $V$  curves measured at different temperature and illumination outdoor conditions. By modeling these data, the electrical parameters were used to indicate the solar radiation and the cell temperature.

The temperature of the cell had been related with the temperature of the absorber using a theoretical expression. The cell temperature can be determined by the inlet temperature and the effective thermal specific power of the collector. The model results fit well with the experimental values, achieving a correlation coefficient of 0.999.

The series resistance was estimated correlating the open circuit resistance against the inverse short circuit current. The average cell series resistance corresponds to the y-interception of the correlation equation.

The model was applied to characterize a PV/T collector. The zero efficiency and heat loss values obtained after applying this process showed a good degree of agreement with the results obtained from the steady-state thermal performance test.

The methodology proposed for the electrical characterization presents more flexibility to obtain the output power for wide range of weather conditions than the model stated in the standard IEC 61215 used for the characterization and certification of photovoltaic modules for terrestrial applications. The proposed model reproduces the photovoltaic module behavior under much more variable working conditions than the international standard and extends the final result application field.

## Acknowledgments

Much appreciated financial support was received from the Ministry of Science and Technology, Spain (MCYT)-(ENE 2010-18357) and the General Directorate of Higher Education (GDHE) of Indonesia.

## References

- [1] Dupeyrat P, Ménézo C, Rommel M, Henning HM. Efficient single glazed flat plate photovoltaic-thermal hybrid collector for domestic hot water system. *Sol Energy* 2011;85:1457–68.
- [2] Kalagirou SA, Tripanagnostopoulos Y. Hybrid PV/T solar systems for domestic hot water and electricity production. *Energy Convers Manage* 2006;47:3368–82.
- [3] Florschuetz LW. Extension of the Hottel-Whiller model to the analysis of combined photovoltaic/thermal flat plate collectors. *Sol Energy* 1979;22:361–6.
- [4] Bernardo LR, Perers B, Håkansson H, Karlsson B. Performance evaluation of low concentrating photovoltaic/thermal systems: a case study from Sweden. *Sol Energy* 2011;85(7):1499–510.
- [5] Chemisana D, Ibañez M, Rosell JI. Characterization of a photovoltaic-thermal module for Fresnel linear concentrator. *Energy Convers Manage* 2011;52(10):3234–40.
- [6] Ji J, Chow TT, He W. Dynamic performance of hybrid photovoltaic/thermal collector wall in Hongkong. *Build Environ* 2003;38:1327–34.
- [7] Chow TT. Performance analysis of photovoltaic-thermal collector by explicit dynamic model. *Sol Energy* 2003;75:143–52.
- [8] Evans DL. Simplified method for predicting photovoltaic array output. *Sol Energy* 1981;27(6):555–60.
- [9] Solanki SC, Dubey S, Tiwari T. Indoor simulation and testing of photovoltaic thermal (PV/T) air collectors. *Appl Energy* 2009;86(11):2421–8.
- [10] Kumar R, Rosen MA. A critical review of photovoltaic-thermal solar collectors for air heating. *Appl Energy* 2011;88(11):3603–14.
- [11] Zondag HA, De Vries DW, Van Helden WGJ, Van Zolingen RJC, Van Steenhoven AA. The thermal and electrical yield of a PV-thermal collector. *Sol Energy* 2002;72(2):113–28.
- [12] Amrizal N, Chemisana D, Rosell JI, Barrau J. A dynamic model based on the piston flow concept for the thermal characterization of solar collectors. *Appl Energy* 2012;94:244–50.
- [13] European Standard EN 12975-2, 2006. CEN, European committee for standardisation; 2006.
- [14] Rosell JI, Ibañez M. Modelling power output in photovoltaic modules for outdoor operating conditions. *Energy Convers Manage* 2006;47:2424–30.
- [15] Mellor A, Domenech-Garret JL, Chemisana D, Rosell JI. A two-dimensional finite element model of front surface current flow in cells under non-uniform, concentrated illumination. *Sol Energy* 2006;83(9):1459–65.
- [16] Chemisana D, Rosell JI. Electrical performance increase of concentrator solar cells under Gaussian temperature profiles; 2011. p. 1205. <http://dx.doi.org/10.1002/pip>.
- [17] Shannon CE. Communication in the presence of noise. *Proc Inst Radio Eng* 1998;37(1):10–21. January, 1949. Reprint as classic paper in: *Proc. IEEE*, 86(2).
- [18] IEC 60904-5. Photovoltaic devices – Part 5: Determination of the equivalent cell temperature (ECT) of photovoltaic (PV) devices by the open-circuit voltage method. Ed. 2.0; 2011.
- [19] IEC 60891. Photovoltaic devices-procedures for temperature and irradiance corrections to measured *I-V* characteristics.
- [20] Del Cueto JA. Method for analyzing series resistance and diode quality factors from field data of photovoltaic modules. *Sol Energy Mater Sol Cells* 1998;55(3):291–7.
- [21] Amrizal N, Chemisana D, Rosell JI. The use of filtering for dynamic characterization of PV/T flat-plate collectors. Eurosun congress, Graz-Austria; 2010.
- [22] IEC 61215:2005. Crystalline silicon terrestrial photovoltaic (PV) modules – design qualification and type approval; 2005.
- [23] Gang P, Huide F, Tao Z, Jie J. A numerical and experimental study on a heat pipe PV/T system. *Solar Energy* 2011;85:911–21.

## ● 21% Overall Similarity

Top sources found in the following databases:

- 20% Internet database
- 9% Publications database
- Crossref database
- Crossref Posted Content database

### TOP SOURCES

The sources with the highest number of matches within the submission. Overlapping sources will not be displayed.

1	<b>ijset.net</b>	Internet	8%
2	<b>iea-shc.org</b>	Internet	4%
3	<b>repositori.udl.cat</b>	Internet	1%
4	<b>Daniel Chemisana, Joan Ignasi Rosell. "Electrical performance increas...</b>	Crossref	1%
5	<b>Fischer, S.. "Collector test method under quasi-dynamic conditions acc...</b>	Crossref	<1%
6	<b>D. Chemisana, M. Ibáñez, J.I. Rosell. "Characterization of a photovoltaic...</b>	Crossref	<1%
7	<b>pure.ulster.ac.uk</b>	Internet	<1%
8	<b>docplayer.net</b>	Internet	<1%
9	<b>nanopdf.com</b>	Internet	<1%

10	<b>hal.archives-ouvertes.fr</b>	Internet	<1%
11	<b>vbn.aau.dk</b>	Internet	<1%
12	<b>backend.orbit.dtu.dk</b>	Internet	<1%
13	<b>members.wto.org</b>	Internet	<1%
14	<b>Vossier, A.. "Very high fluxes for concentrating photovoltaics: Consider...</b>	Crossref	<1%
15	<b>Tonui, J.K.. "Improved PV/T solar collectors with heat extraction by for...</b>	Crossref	<1%
16	<b>hdl.handle.net</b>	Internet	<1%
17	<b>mdpi-res.com</b>	Internet	<1%
18	<b>tdx.cat</b>	Internet	<1%
19	<b>ssl.mit.edu</b>	Internet	<1%
20	<b>sumproject.eu</b>	Internet	<1%
21	<b>Perers, B.. "Dynamic method for solar collector array testing and evalu...</b>	Crossref	<1%

22	<b>bura.brunel.ac.uk</b>	Internet	<1%
23	<b>tel.archives-ouvertes.fr</b>	Internet	<1%
24	<b>ebd.lth.se</b>	Internet	<1%
25	<b>jree.ir</b>	Internet	<1%
26	<b>dehesa.unex.es:8080</b>	Internet	<1%
27	<b>komagome.tkl.iis.u-tokyo.ac.jp</b>	Internet	<1%
28	<b>ore.exeter.ac.uk</b>	Internet	<1%
29	<b>ro.uow.edu.au</b>	Internet	<1%
30	<b>worldwidescience.org</b>	Internet	<1%
31	<b>researchgate.net</b>	Internet	<1%

## ● Excluded from Similarity Report

- Submitted Works database
- Quoted material
- Small Matches (Less than 8 words)
- Manually excluded text blocks
- Bibliographic material
- Cited material
- Manually excluded sources

### EXCLUDED SOURCES

<b>coek.info</b>	<b>78%</b>
Internet	
<b>N. Amrizal, D. Chemisana, J.I. Rosell. "Hybrid photovoltaic-thermal solar colle...</b>	<b>73%</b>
Crossref	
<b>tesisenred.net</b>	<b>70%</b>
Internet	
<b>Amrizal, N., D. Chemisana, and J.I. Rosell. "Hybrid photovoltaic&amp;quot;thermal sol...</b>	<b>69%</b>
Crossref	
<b>N. Amrizal, D. Chemisana, J.I. Rosell, J. Barrau. "A dynamic model based on t...</b>	<b>9%</b>
Crossref	
<b>Amrizal, N.. "A dynamic model based on the piston flow concept for the therm...</b>	<b>8%</b>
Crossref	
<b>D. Chemisana, J.I. Rosell, A. Riverola, Chr. Lamnatou. "Experimental performa...</b>	<b>1%</b>
Crossref	
<b>Chemisana, D., J.I. Rosell, A. Riverola, and Chr. Lamnatou. "Experimental perf...</b>	<b>1%</b>
Crossref	
<b>Karim Menoufi, Daniel Chemisana, Joan I. Rosell. "Life cycle assessment of a ...</b>	<b>1%</b>
Crossref	

<b>Farah Ramadhani, M.A. Hussain, Hazlie Mokhlis, Hazlee Azil Illias. "Optimal h...</b>	<b>1%</b>
Crossref	
<b>D. Chemisana, Chr. Lamnatou. "Photovoltaic-green roofs: An experimental ev...</b>	<b>&lt;1%</b>
Crossref	
<b>foitic.itenas.ac.id</b>	<b>&lt;1%</b>
Internet	
<b>isiarticles.com</b>	<b>&lt;1%</b>
Internet	
<b>Vassiliki Drosou, Loreto Valenzuela, Argiro Dimoudi. "A new TRNSYS compon...</b>	<b>&lt;1%</b>
Crossref	
<b>Renewable Energy in the Service of Mankind Vol II, 2016.</b>	<b>&lt;1%</b>
Crossref	
<b>"Renewable Energy in the Service of Mankind Vol II", Springer Science and Bu...</b>	<b>&lt;1%</b>
Crossref	
<b>eproceeding.itenas.ac.id</b>	<b>&lt;1%</b>
Internet	
<b>repository.lppm.unila.ac.id</b>	<b>&lt;1%</b>
Internet	
<b>Abdelkrim Khelifa, Khaled Touafek, Boutina Lyes, Mouhamed Tahar Baissi. "N...</b>	<b>&lt;1%</b>
Crossref	
<b>Tanweer, Bilal. "Modeling and Performance Analysis of Low Concentration Ph...</b>	<b>&lt;1%</b>
Publication	
<b>Madaci, Bouthaina, Rachid Chenni, Erol Kurt, and Kamel Eddine Hemsas. "Desi...</b>	<b>&lt;1%</b>
Crossref	

**Jie Deng, Ming Yang, Rongjiang Ma, Xiaolin Zhu, Jianhua Fan, Guofeng Yuan, ...** <1%

Crossref

---

**Li Xu, Zhifeng Wang, Xin Li, Guofeng Yuan, Feihu Sun, Dongqiang Lei, Shidong...** <1%

Crossref

---

**Magalhaes, Pedro Mendes de Lacerda Peixoto de. "Study of Pump Control in ...** <1%

Publication

---

**Zhiyong Tian, Bengt Perers, Simon Furbo, Jianhua Fan. "Thermo-economic op...** <1%

Crossref

---

**Zhiyong Tian, Bengt Perers, Simon Furbo, Jianhua Fan. "Analysis and validatio...** <1%

Crossref

---

**Zhiyong Tian, Bengt Perers, Simon Furbo, Jianhua Fan. "Analysis and validatio...** <1%

Crossref

---

**Wei Pang, Qian Zhang, Yanan Cui, Linrui Zhang, Hongwen Yu, Xiaoyan Zhang, ...** <1%

Crossref

---

**Lin, Jian, Tianjun Liao, and Bihong Lin. "Performance analysis and load matchi...** <1%

Crossref

---

**Richárd Kicsiny. "Multiple linear regression based model for solar collectors", ...** <1%

Crossref

---

**Wei Pang, Yanan Cui, Qian Zhang, Gregory.J. Wilson, Hui Yan. "A comparative ...** <1%

Crossref

---

**Aminu Yusuf, Nevra Bayhan, Hasan Tiryaki, Bejan Hamawandi, Muhammet S. ...** <1%

Crossref

---

**Primož Poredoš, Urban Tomc, Nada Petelin, Boris Vidrih, Uroš Flisar, Andrej Ki...** <1%

Crossref

---

**Khelifa, Abdelkrim, Khaled Touafek, and Hocine Ben Moussa. "Approach for t... <1%**

Crossref

---

**Abdelkrim Khelifa, Khaled Touafek, Hocine Ben Moussa. "Approach for the m... <1%**

Crossref

---

**Michael, Jee Joe, and S. Iniyar. "Performance analysis of a copper sheet lami... <1%**

Crossref

---

**Riccardo Simonetti, Luca Molinaroli, Giampaolo Manzolini. "Development and ... <1%**

Crossref

---

**Thomas Foken. "Micrometeorology", Springer Science and Business Media LL... <1%**

Crossref

#### EXCLUDED TEXT BLOCKS

**Applied Energy 101 (2013**

repozitorij.fsb.hr

---

**A hybrid photovoltaic/thermal transient model has been developed and validated e...**

www.cheric.org

---

**highlights" A hybrid photovoltaic/thermal dynamic model is presented." The model...**

worldwidescience.org